

AD-A045 994

FOREIGN TECHNOLOGY DIV WRIGHT-PATTERSON AFB OHIO  
THE CALCULATION OF INCLUSIVE GAMMA SPECTRA AT HIGH ENERGIES, (U)  
JUN 77 R BLUTNER, S FRANK, K HAENSGEN, H THAN  
FTD-ID(RS)T-0900-77

F/G 20/8

UNCLASSIFIED

| OF |

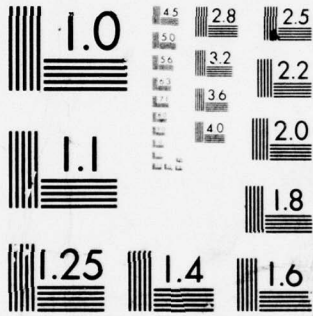
AD  
A045994



NL



END  
DATE  
FILMED  
11-77  
DDC



MICROCOPY RESOLUTION TEST CHART  
NATIONAL BUREAU OF STANDARDS-1963-A

1

AD-A045994

FOREIGN TECHNOLOGY DIVISION



THE CALCULATION OF INCLUSIVE GAMMA SPECTRA  
AT HIGH ENERGIES

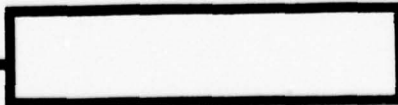
by

R. Blutner, S. Frank, et al.



DDC  
RECEIVED  
NOV 7 1977  
D

Approved for public release;  
distribution unlimited.



ACCESSION for	
RTIS	White Section <input checked="" type="checkbox"/>
DDG	Buff Section <input type="checkbox"/>
UNANNOUNCED	<input type="checkbox"/>
JUSTIFICATION.....	
BY.....	
DISTRIBUTION/AVAILABILITY CODES	
Dist.	AVAIL. REQ./BY SPECIAL
<b>A</b>	

FTD ID(RS)T-0900-77

## EDITED TRANSLATION

FTD-ID(RS)T-0900-77      14 June 1977  
 MICROFICHE NR: *FTD-77-C-000704*

CSL76032824

THE CALCULATION OF INCLUSIVE GAMMA SPECTRA AT HIGH ENERGIES

By: R. Blutner, S. Frank, et al.

English pages: 17

Source: Wissenschaftliche Zeitschrift, Mathematisch-Naturwissenschaftliche Reihe, Karl-Marx-Universität Leipzig, Volume 21, Number 4, 1972, PP. 409-419.

Country of origin: East Germany

Translated by: SCITRAN

F33657-76-D-0390

Requester: FTD/ETDP

Approved for public release; distribution unlimited.

<p>THIS TRANSLATION IS A RENDITION OF THE ORIGINAL FOREIGN TEXT WITHOUT ANY ANALYTICAL OR EDITORIAL COMMENT. STATEMENTS OR THEORIES ADVOCATED OR IMPLIED ARE THOSE OF THE SOURCE AND DO NOT NECESSARILY REFLECT THE POSITION OR OPINION OF THE FOREIGN TECHNOLOGY DIVISION.</p>	<p>PREPARED BY:           TRANSLATION DIVISION          FOREIGN TECHNOLOGY DIVISION          WP-AFB, OHIO.</p>
---	--

FTD ID(RS)T-0900-77

Date 14 June 19 77

THE CALCULATION OF INCLUSIVE GAMMA SPECTRA AT  
HIGH ENERGIES (1)

R. Blutner, S. Frank, K. Hänsgen, Htun Than, H. König,  
J. Kripfganz, H. Kühnicke, H. Lemke, H. J. Möhring, V. Müller,  
G. Ranft, J. Ranft and F. Thiel

1. Introduction

Gamma quanta which are produced in highly energetic  $pp$  or  $\pi p$  collisions arise almost exclusively from the decomposition of the  $\pi^0$  mesons which are produced first:



This fact makes it possible to find the differential effective cross section of the  $\gamma$  quanta produced by purely kinematic calculations from a known  $\pi^0$  spectrum. The  $\pi^0$  spectrum is calculated according to the thermodynamic model [2, 4, 5, 6, 7, 9, 10]. This takes both of the essential possibilities for production of  $\pi^0$  mesons into consideration:

- The  $\pi^0$  arises through direct decomposition of a fireball.
- The fireball is considered as a resonance. This resonance decomposes into  $\pi^0$  and  $p$ .

In Section 2 we calculate, for the special case of isotropic

---

(1) This work was produced under the care of Professors G. Ranft and J. Ranft by a student group consisting of 7 second and third year students (as part of the WPS), 2 graduates, one research student and one aspirant. At the Exhibition of The Karl Marx University, Leipzig, 1972, it was distinguished with the Prize of the Karl Marx University, 1st Stage.

$\pi^0$  spectra an expression for the differential effective cross section of the  $\gamma$  quanta.

For the general case of anisotropic  $\pi^0$  distributions we give in Section 3 a Monte Carlo method with which the  $\gamma$  spectra can be calculated. In order to determine the  $\gamma$  spectra with good statistics, however, the Monte Carlo program requires a substantial computer time. Therefore, in Sections 4 (direct production of the  $\pi^0$ ) and 5 (production of the  $\pi^0$  through resonance) the spectrum is in part analytically calculated. Our results are reported in Section 6 and discussed in comparison with the existing experimental data.

## 2. The Calculation of $\gamma$ -Spectra from Isotropic $\pi^0$ Spectra

Let an unstable particle of mass  $m$  be generated in a collision between particles  $a$  and  $b$ . Let the momentum spectrum of this particle be isotropic in the center of gravity system; that is,

$$\frac{d^3\sigma}{d^3\vec{p}} = \tilde{f}(|\vec{p}|) = \tilde{f}(p) = \tilde{f}(\epsilon^2 - m^2) = f(\epsilon). \quad (2.1)$$

Let the particle of mass  $m$  decompose into particles  $l^*$  and  $j$  with masses  $m_l$  and  $m_j$ . We seek the momentum spectrum  $f_l(\epsilon)$  of the particle  $l$  in the center of gravity system.

Under the assumption that the unstable particle disintegrates isotropically,  $f_l(\epsilon)$  can be determined from purely kinematic considerations. These calculations are presented in [3]. If, instead of the momentum distributions  $f_l(\epsilon)$  and  $f_j(\epsilon)$  one introduces the energy distributions

$$\begin{aligned} \omega(\epsilon^*) &= 4\pi p^* \epsilon^* f(\epsilon^*) \\ \omega_l(\epsilon) &= 4\pi p \epsilon f_l(\epsilon) \end{aligned} \quad (2.2)$$

[Throughout the document  $l = \text{Italic } l$ .]

then the result is

$$\omega_l(\epsilon) = \frac{m^*}{2p_l} \int_{\epsilon_-^*}^{\epsilon_+^*} d\epsilon^* \frac{\omega(\epsilon^*)}{\sqrt{\epsilon^{*2} - m^{*2}}} \quad (2.3)$$

with

$$\begin{aligned} \epsilon_*^* &= \frac{m^*}{m_l^2} (\epsilon \epsilon_l \pm p p_l) \\ \epsilon_l &= \frac{m^{*2} + (m_l^2 - m_j^2)}{2m^*} \\ p_l^2 &= \epsilon_l^2 - m_l^2 = \frac{[m^{*2} - (m_l + m_j)^2] [m^{*2} - (m_l - m_j)^2]}{4m^{*2}} \end{aligned} \quad (2.4)$$

These relations, however, apply only if the rest masses of particles 1 and j are finite ( $m_l \neq 0, m_j \neq 0$ ).

On disintegration of the unstable particle of mass m into particles 1 and j with vanishing rest mass (e. g.,  $\gamma$  quanta, a limit transition is necessary,  $m_l = m_j = m \rightarrow 0$ ). This limit transition gives, for the limits, instead of the expression (2.4)

$$\begin{aligned} \epsilon_-^* &= \epsilon + \frac{m^{*2}}{4\epsilon} \\ \epsilon_+^* &\rightarrow \infty. \end{aligned} \quad (2.5)$$

For finite collision energy, we must use instead of  $\epsilon_+^* \rightarrow \infty$  the maximum possible energy of the unstable particle:

$$\epsilon_+^* = \epsilon_{\max}^* \quad (2.6)$$

### 3. The Monte Carlo Procedure

If the momentum distribution of the unstable particle of mass  $m$  is anisotropic, then (2.3) must be replaced by a considerably more complex multiple integral which can be evaluated only by means of drastic approximations (e. g., [11]) or tedious numerical calculations. In this case it is simpler to calculate the  $\gamma$  spectrum using a Monte Carlo procedure.

In the Monte Carlo procedure the scattering or disintegration process is simulated in a computer. Here we consider the decomposition  $\pi^0 \rightarrow 2\gamma$ . The  $\pi^0$  spectra can be specified in arbitrary form (e. g., from an empirical formula, or according to the thermodynamic model [2, 4, 5, 6, 7, 9, 10]). Corresponding to the selected statistics, from this one determines the number of  $\pi^0$  mesons which vanish in a single phase space element. In the rest system of the  $\pi^0$  the disintegration  $\pi^0 \rightarrow 2\gamma$  is isotropic ( $\pi^0$  has zero spin). The disintegration angle is a free parameter and in the Monte Carlo procedure it is occupied by random numbers. Then the disintegration is unambiguously defined. The momentum of the  $\gamma$  quanta is transformed back to the starting system. Corresponding to the phase space decomposition, the  $\gamma$  quanta are assigned to their phase space elements. Thus one obtains the  $\gamma$  distribution as a histogram.

### 4. $\gamma$ Spectra According to the Thermodynamic Model; the Contribution of Directly Generated $\pi^0$ Mesons

For the thermodynamic calculation of the contribution to the  $\gamma$  spectra resulting from the disintegration of directly generated  $\pi^0$  mesons we need the function  $f^0(\epsilon, T)$ . This function designates the momentum distribution of the  $\gamma$  quanta arising from directly generated  $\pi^0$  mesons. Here, the reference system for the resting system is a fireball of temperature  $T$ .

According to the thermodynamic model [2, 4, 5, 7, 10] the spectrum of the directly generated  $\pi^0$  mesons in the resting system of the fireball is isotropic:

$$f(\epsilon^*) = \frac{z^* V}{8\pi^3} \cdot \frac{1}{e^{\epsilon^*/T} - 1}. \quad (4.1)$$

In the following, we neglect the one in the denominator. If the  $\pi^0$  disintegrates isotropically into particles of mass  $m_1$  and  $m_j$ , then an elementary calculation of the integral (2.3) gives

$$f_i(\epsilon) = \frac{m^* z^* z_1 V}{16\pi^3 p_1 p \epsilon} T^2 \left[ \left(1 + \frac{\epsilon^*}{T}\right) e^{-(\epsilon^*/T)} - \left(1 + \frac{\epsilon_j^*}{T}\right) e^{-(\epsilon_j^*/T)} \right]. \quad (\text{cf. [3]}) (4.2)$$

Here  $m^*$  is the mass of the unstable particle (in our case, of the  $\pi^0$  meson);  $z_1$  and  $z^*$  are the multiplicities of the particles with masses  $m_1$  and  $m^*$ , respectively.  $f^0(\epsilon, T)$ ,  $\epsilon^*$ ,  $\epsilon_j^*$  and  $p_1$  are given in Formula (2.4). The  $\gamma$  spectrum in the rest system of a fireball arises through the limit transition  $m_i = m_j = m \rightarrow 0$ .

As is shown in Section 2, in (4.2) we must use for  $\epsilon^*$  and  $\epsilon_j^*$  the expressions (2.5) and (2.6), respectively:

$$f_i^0(\epsilon, T) = \frac{z^* V}{8\pi^3 \epsilon^2} T^2 \left[ \left(1 + \frac{\epsilon^*}{T}\right) e^{-(\epsilon^*/T)} - \left(1 + \frac{\epsilon_j^*}{T}\right) e^{-(\epsilon_j^*/T)} \right]. \quad (4.3)$$

## 5. $\gamma$ -Spectra According to the Thermodynamic Model; The Contribution of $\pi^0$ Mesons Generated by the Decomposition of Continuous Resonances

### 5.1 Formulation of the problem and transformation of the integral

We need the function  $f^R(\epsilon, T)$ , which is the analog of the function  $f^0(\epsilon, T)$ . But here the  $\pi^0$  mesons are generated by the decomposition of a continuous resonance. Thus, we consider the disintegration scheme in (1). In order to obtain the

momentum spectrum of the  $\pi^0$  mesons from (4.2), we set there:

$$\begin{aligned} m_i &= m_\pi \\ m_j &= m_p \\ m^* &= \text{mass of the resonance} \end{aligned} \quad (5.1)$$

The momentum spectrum  $f_\gamma^R(\varepsilon, T)$  of the  $\gamma$  quanta in the rest system of a fireball arises from this through a further integration of (2.3) and (2.4). Then we perform the limit transition  $m_j \rightarrow 0$  :

$$f_\gamma^R(\varepsilon, T) = \frac{z_\gamma z_\pi z^* m^* V}{16\pi^3 p_\pi \varepsilon^2} T^2 \int_{\varepsilon_-}^{\varepsilon_+} \frac{d\omega}{\sqrt{\omega^2 - m_\pi^2}} \left[ \left(1 + \frac{W_-}{T}\right) e^{-(W_-/T)} - \left(1 + \frac{W_+}{T}\right) e^{-(W_+/T)} \right] \quad (5.2)$$

$$\begin{aligned} \varepsilon_+ &= \varepsilon_{\max} \\ \varepsilon_- &= \varepsilon + \frac{m_\pi^2}{4\varepsilon} = m\pi + \frac{1}{\varepsilon} \left( \varepsilon - \frac{m\pi}{2} \right)^2 \\ W_\pm &= \frac{m^*}{m_\pi^2} (\omega \varepsilon_\pi \pm \sqrt{\omega^2 - m_\pi^2} \sqrt{\varepsilon_\pi^2 - m_\pi^2}) \end{aligned} \quad (5.3)$$

$$\varepsilon_\pi = \frac{m^{*2} + m_\pi^2 - m_p^2}{2m^*} \quad (5.4)$$

Next, we must calculate the integral (5.2). We introduce the following designations:

$$I_\mp(\varepsilon) = \int_{\varepsilon_-}^{\varepsilon_+} \frac{d\omega}{\sqrt{\omega^2 - m_\pi^2}} \left(1 + \frac{W_\mp}{T}\right) e^{-(W_\mp/T)} \quad (5.5)$$

Because  $\varepsilon_- \geq m_\pi$  and  $\varepsilon_+ = m_\pi$ , only if  $\varepsilon = m_\pi/2$ , then for  $\varepsilon \neq m_\pi/2$  the integrand in (5.5) is a continuous function in the range of integration. The substitution

$$\begin{aligned} \frac{\omega}{m_\pi} &= \cos hz \\ \frac{\varepsilon_\pi}{m_\pi} &= \cos ha \end{aligned} \quad (5.6)$$

yields

$$I_{\mp} = \int_{z(\epsilon_-)}^{z(\epsilon_+)} dz \left[ 1 + \frac{m^*}{T} \cos h(z \mp a) \right] e^{-(m^*/T) \cos h(z \mp a)} \quad (5.7)$$

A further substitution

$$\begin{aligned} I_- : \cos h(z - a) &= y_- \\ I_+ : \cos h(z + a) &= y_+ \end{aligned} \quad (5.8)$$

gives

$$I_{\mp} = \int_{y_{\mp}(\epsilon_-)}^{y_{\mp}(\epsilon_+)} \frac{1}{\sqrt{1 - (1/y^2)}} \left( \frac{m^*}{T} + \frac{1}{y} \right) e^{-(m^*/T)y} dy \quad (5.9)$$

The function  $y_{\pm}(\omega) = \cos h(z(\omega) \mp a)$  has the form

$$y_{\mp}(\omega) = \frac{\omega}{m_{\pi}} \frac{\epsilon_{\pi}}{m_{\pi}} \mp \sqrt{\frac{\omega^2}{m_{\pi}^2} - 1} \sqrt{\frac{\epsilon_{\pi}^2}{m_{\pi}^2} - 1} \quad (5.10)$$

At the lower limit this expression simplifies to

$$\begin{aligned} y_-(\epsilon_-) &= \frac{\epsilon}{m_{\pi}} v + \frac{m_{\pi}}{4\epsilon} u \quad \text{falls } \epsilon > m_{\pi}/2 \\ y_-(\epsilon_-) &= \frac{\epsilon}{m_{\pi}} u + \frac{m_{\pi}}{4\epsilon} v \quad \text{falls } \epsilon \leq m_{\pi}/2 \\ y_+(\epsilon_-) &= \frac{\epsilon}{m_{\pi}} u + \frac{m_{\pi}}{4\epsilon} v \quad \text{falls } \epsilon > m_{\pi}/2 \\ y_+(\epsilon_-) &= \frac{\epsilon}{m_{\pi}} v + \frac{m_{\pi}}{4\epsilon} u \quad \text{falls } \epsilon \leq m_{\pi}/2 \end{aligned} \quad (5.11)$$

at

$$\begin{aligned} v &= \frac{\epsilon_{\pi}}{m_{\pi}} - \sqrt{\left(\frac{\epsilon_{\pi}}{m_{\pi}}\right)^2 - 1} \\ u &= \frac{\epsilon_{\pi}}{m_{\pi}} + \sqrt{\left(\frac{\epsilon_{\pi}}{m_{\pi}}\right)^2 - 1} \end{aligned} \quad (5.12)$$

We always have

$$y_{\mp}(\epsilon_{-}) \geq 1.$$

If  $I(a, b)$  designates the integral (5.9) with the lower limit  $a$  and the upper limit  $b$ , then we must solve this integral for  $\infty > b > a \geq 1$ .

## 5.2 Analytical Solution

If the lower limit in (5.9) is large, then it is a good approximation to expand the root in the denominator as follows:

$$\left(1 - \frac{1}{y^2}\right)^{-1/2} \sim 1 + \frac{1}{2y^2}. \quad (5.13)$$

With this, (5.9) gives

$$I_A(a, b) = \int_a^b \left( \frac{m^*}{T} + \frac{1}{y} + \frac{m^*}{2Ty^2} + \frac{1}{2y^3} \right) e^{-(m^*/T)y} dy. \quad (5.14)$$

By virtue of the relations

$$\int_x^\infty \frac{e^{-(m^*/T)y}}{y} dy = -E_1\left(\frac{m^*}{T}x\right), \quad (5.15)$$

where  $E_1(x)$  is the exponential integral and

$$\int \frac{e^{-(m^*/T)y}}{y^n} dy = \frac{1}{n-1} \left( -\frac{e^{-(m^*/T)y}}{y^{n-1}} - \frac{m^*}{T} \int \frac{e^{-(m^*/T)y}}{y^{n-1}} dy \right), \quad (5.16)$$

it is possible to calculate the integral (5.14):

$$I_A(a, b) = \left[ e^{-(m^*/T)y} \left( 1 + \frac{m^*}{4Ty} + \frac{1}{4y^2} \right) - E_1\left(\frac{m^*}{T}y\right) \left( \frac{m^{*2}}{4T^2} - 1 \right) \right]_a^b. \quad (5.17)$$

One can easily estimate that for  $a > 1.4$  the error arising from the approximation (5.13) is less than 15%.

### 5.3 Numerical Solution

For  $a < 1.4$  the approximation (5.13) cannot be used. In order to bring expression (5.9) into a suitable form for numerical calculations, we substitute here

$$y^2 - 1 = x^2 \quad (5.18)$$

and obtain

$$I_N(a, b) = \int_{\sqrt{a^2-1}}^{\sqrt{b^2-1}} dx \left( \frac{m^*}{T} + \frac{1}{\sqrt{x^2-1}} \right) e^{-(m^*/T)\sqrt{1+x^2}}. \quad (5.19)$$

In order that the integrand not vary excessively, it is desirable to divide the term  $(m^*/T)e^{-(m^*/T)\sqrt{1+x^2}}$  additively:

$$I_N(a, b) = w(a, b) + II_N(a, b) \quad (5.20)$$

at

$$\begin{aligned} w(a, b) &= \int_{\sqrt{a^2-1}}^{\sqrt{b^2-1}} dx \frac{m^*}{T} e^{-(m^*/T)\sqrt{1+x^2}} = \sqrt{\frac{\pi}{2}} \sqrt{\frac{m^*}{T}} e^{-(m^*/T)} \left[ \operatorname{erf} \left( \sqrt{\frac{m^*}{T}} x \right) \right]_{\sqrt{a^2-1}}^{\sqrt{b^2-1}} \\ II_N(a, b) &= \int_{\sqrt{a^2-1}}^{\sqrt{b^2-1}} dx \\ &\times \left[ \frac{m^*}{T} (e^{-(m^*/T)\sqrt{1+x^2}} - e^{-(m^*/T)\sqrt{1+(x^2/2)}}) + \frac{1}{\sqrt{x^2+1}} e^{-(m^*/T)\sqrt{1+x^2}} \right]. \end{aligned} \quad (5.22)$$

Here  $\operatorname{erf}(z) = \frac{2}{\sqrt{\pi}} \int_0^z e^{-t^2} dt$  is the error function. The main part of  $w(a, b)$  appears in (5.20) if  $a$  and  $b$  are near 1.

## 5.4 Summary

In the calculation of the  $\gamma$  spectrum in the rest system of the fireball (5.2) the integral (5.9)

$$I_-(y_-(\epsilon_-), y_-(\epsilon_+)) \quad \text{and} \quad I_+(y_+(\epsilon_-), y_+(\epsilon_+))$$

must be solved. Depending on the positions of the lower limit,  $a$ , and the upper limit,  $b$ , we can distinguish 3 cases:

Case 1:  $1.4 = uu \leq a < b$

Formula (5.17) is used with an error less than 15%.

Case 2.  $1 \leq a < b \leq uu = 1.4$

(5.20) is used.  $I_N(a, b)$  (5.22) here must be calculated numerically using a Gaussian integration formula.

If the upper integration limit here is far above the lower, then one can arbitrarily reduce the upper limit without making a large error. But the error occurring in the numerical integration is smaller.

Let us calculate

$$\begin{aligned} \text{a) } m^*/T(b-a) < D \quad (D \text{ specified } \approx 4) \\ I_N(a, b) &= w(a, b) + II_N(a, b) \\ \text{b) } m^*/T(b-a) > D \end{aligned} \quad (5.23)$$

Set  $b = T/m^* D + a$  and calculate

$$I_N(a, b) = w(a, b) + II_N(a, b). \quad (5.24)$$

The error remains smaller than  $e^{-D} \cdot 100\%$ .

Case 3.  $1 \leq a \leq uu = 1.4 \leq b$

This case is reduced to cases 1 and 2:

$$I(a, b) = I_N(a, uu) + I_N(uu, b) \quad (5.25)$$

The function (5.2)  $f_\gamma^R(\epsilon, T)$  for  $\pi^0$  generated by resonance disintegration is computed numerically using the formulas above by means of a FORTRAN program. Using the program SPUK [9] a contribution to the differential effective cross section for  $\gamma$  production is calculated from this. The other contribution arises from the function  $f_\gamma^0(\epsilon, T)$  (Formula (4.3)). Both contributions, added, give the differential momentum spectrum for  $\gamma$  production.

## 6. Results and Discussion

The version of the thermodynamic model based on the "strong bootstrap solution" (see [6]) is used for the thermodynamic calculation of the  $\gamma$  spectra. The free parameters of the model are adapted to 19 to 70 GeV/c data from pp collisions. We assume that the observed  $\gamma$  spectra can be completely explained from the decomposition of  $\pi^0$  mesons. Our results indicate that this assumption is apparently justified. The thermodynamic parameters for the reaction  $p + p \rightarrow \pi^0 + \dots$  are needed for the calculation of the  $\gamma$  spectra. As there are neither thermodynamic calculations nor experimental data for this reaction, we use in place of the  $\pi^0$  spectra the thermodynamic  $\pi^+$  or  $\pi^-$  spectra. In Figure 1, the  $\gamma$  spectra calculated with the Monte Carlo procedure (Section 3) in the form  $\delta^2 N / \delta p d\Omega$  in the center of gravity system are compared with the experimental data [1] for the reaction  $p + p \rightarrow \gamma + \dots$  at 23.1 GeV. For the calculation of the thermodynamic  $\gamma$  spectra

it is assumed that the  $\pi^0$  spectra are identical with the  $\pi^+$  spectra. Figure 2 shows the comparison of the same data with the direct thermodynamic calculation which was described in Sections 4 and 5. Here it was assumed that the  $\pi^0$  spectra are identical with the  $\pi^-$  spectra.

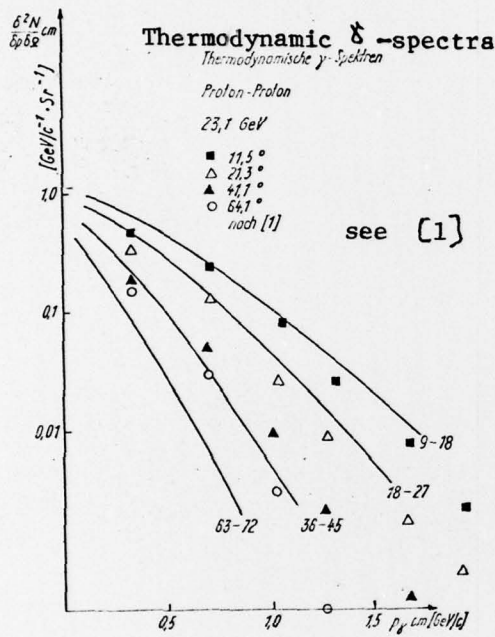


Figure 1. Comparison of the experimental  $\gamma$  spectra [1] in the form  $(\partial^2 N / \partial p \partial \Omega) \text{ cm}$  at  $p_{\perp ab} = 23,1 \text{ GeV}/c$  with the thermodynamically calculated  $\gamma$  spectra. The Monte Carlo method was used for the calculation. We used  $\pi^+$  spectra instead of the  $\pi^0$  spectra.

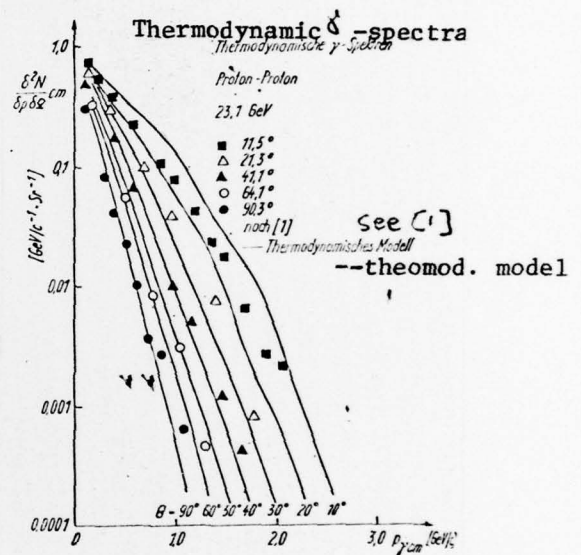


Figure 2. Comparison of the experimental  $\gamma$  spectra [1] in the form  $(\partial^2 N / \partial p \partial \Omega) \text{ cm}$  at  $p_{\perp ab} = 23,1 \text{ GeV}/c$  with the thermodynamically calculated  $\gamma$  Spectra. The analytical method was used for the calculation. We used  $\pi^-$  spectra instead of the  $\pi^0$  spectra.

Inclusive  $\gamma$  spectra  $p + p \rightarrow \gamma + \dots$  were measured in an ISR experiment [8]. The collision energy corresponded to laboratory momenta of up to 1,500 GeV/c. Figures 3 and 4 show the comparison of these data in the form  $\partial^2 N / \partial p \partial \Omega$  in the center of gravity system with the analytically calculated  $\gamma$  spectra. It is likewise assumed that the  $\pi^0$  spectra are identical with the  $\pi^-$  spectra. In Figure 5, one of the measured curves at  $E_{\text{cm}} = 52.7$  GeV is compared with the result of the Monte Carlo method; as in Figure 1 the  $\pi^0$  spectra are assumed to be identical with the  $\pi^+$  spectra. In Figure 6, the data at  $E_{\text{cm}} = 52.7$  GeV in the form  $E(d^3N/d^3p)$  at  $p_{\parallel} = 0$  are compared with the results of the Monte Carlo calculation.

We could establish that both methods for calculating the inclusive  $\gamma$  spectra according to the thermodynamic model yield consistent results, as can be seen from the calculated spectra at 23.1 GeV in Figures 1 and 2, and at 1,500 GeV in Figures 4 and 5. We find that the experimental data at 23.1 GeV approximately coincide with the calculated values. The deviations may be explained from the fact that we used the thermodynamic  $\pi^-$  or  $\pi^+$  spectra instead of the  $\pi^0$  spectra. At large angles, the major contribution to the spectra comes from the directly produced  $\pi^0$  (Section 4). At smaller angles the contribution from  $\pi^0$  produced in continuous resonances, calculated in Section 5, increases.

The thermodynamic calculation of the  $\gamma$  spectra at 1,000 and 1,500 GeV and the comparison with the ISR data is significant for the following reasons:

- Conclusions about the  $\pi^0$  spectra at these high energies can be drawn from the  $\gamma$  spectra.
- The  $\gamma$  spectra are measured up to angles of  $90^\circ$  in the center of gravity system. The model is compared with experimental data for the first time at energies up to 1,500 GeV in the central region.

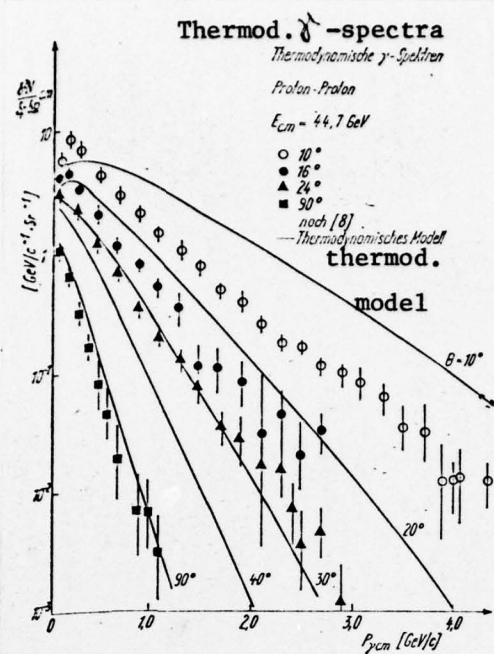


Figure 3. Comparison of the  $\gamma$  spectra measured by ISR [8] in the form  $(\frac{\partial^2 N}{\partial p \partial \Omega})_{cm}$  at  $E_{cm} = 44.7 \text{ GeV}$  with the thermodynamically calculated  $\gamma$  spectra. The analytical method was used for the calculation. We used  $\pi^-$  spectra instead of the  $\pi^0$  spectra.

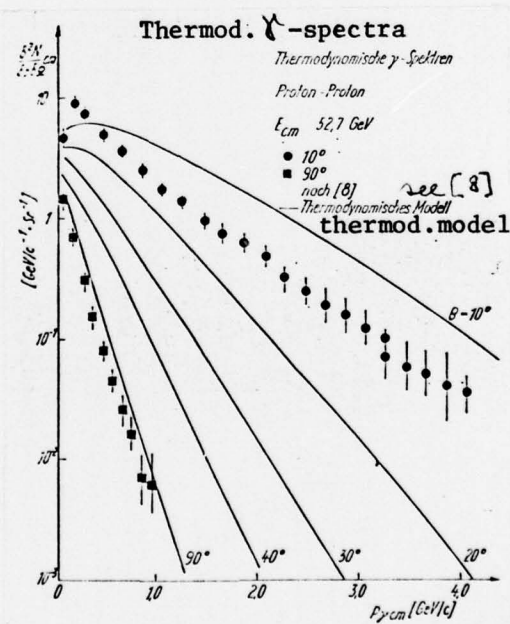


Figure 4. Comparison of the inclusive  $\gamma$  spectra measured by ISR [8] in the form  $(\frac{\partial^2 N}{\partial p \partial \Omega})_{cm}$  at  $E_{cm} = 52.7 \text{ GeV}$  for a scattering angle of  $\theta_{cm} = 10, 2^\circ, 90^\circ$  with the thermodynamically calculated  $\gamma$  spectra. The analytical method was used for the calculation. We used  $\pi^-$  instead of the  $\pi^0$  spectra.

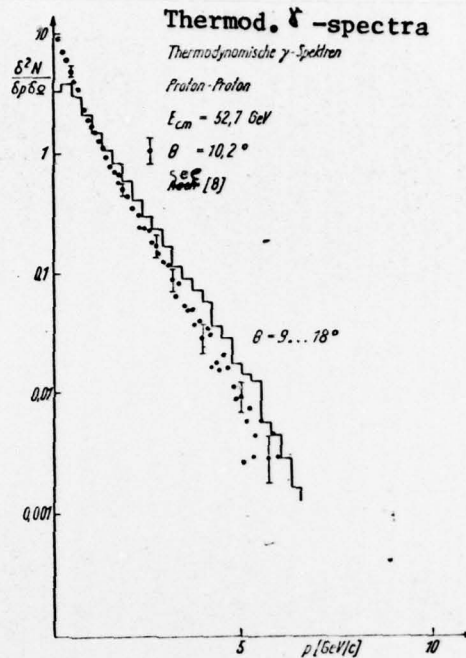


Figure 5. Comparison of the inclusive  $\gamma$  spectra [8] measured by ISR in the form  $(\frac{\delta^2 N}{\delta p \delta \Omega})$  for  $\theta = 10.2^\circ$  at an energy  $E_{cm} = 52.7$  GeV with the thermodynamically calculated  $\gamma$  spectra. The Monte Carlo method was used for the calculation. We used  $\pi^+$  spectra instead of the  $\pi^0$  spectra.

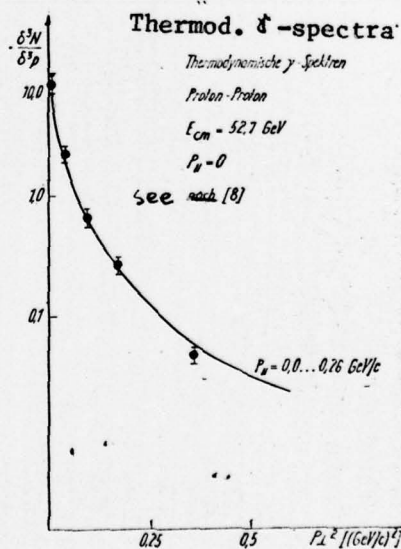


Figure 6. Comparison of the inclusive  $\gamma$  spectra [8] measured by ISR in the form  $E \cdot (\frac{\delta^3 N}{\delta^3 p})$  as a function of  $p_1^2$  for  $p_{11} \sim 0$  at an energy of  $E_{cm} = 52.7$  GeV with the thermodynamically calculated  $\gamma$  spectra. The Monte Carlo method was used for the calculation. We used  $\pi^+$  instead of  $\pi^0$  spectra.

- The thermodynamic  $\pi^+$  and  $\pi^-$  spectra are compared at energies of 19 to 70 GeV with the data. It is shown in [6] that, for small angles and energies of 500 to 1,500 GeV, the extrapolated thermodynamic spectra, including their absolute standardization, approximately agree with the ISR data for inclusive  $\pi^+$  or  $\pi^-$  production. In our work, likewise, the  $\gamma$  spectra, including their absolute standardization, are predicted in the entire kinematically possible range and compared with experimental data in a significantly larger angular range than in the case of the  $\pi^+$  spectra.

Figures 3 to 6 show approximate agreement with the experiment. It follows from the agreement obtained that for these energies and the angles considered the differences between the  $\pi^+$ ,  $\pi^-$  and  $\pi^0$  spectra are apparently slight. The thermodynamic spectra show "scaling" behavior and a non-vanishing central plateau [6]. It follows from the comparison with the  $\gamma$  data that the  $\pi^0$  spectra in the fragmentation and pionization region apparently also show at least approximate "scaling" behavior. The deviations which occur between the thermodynamic  $\gamma$  spectra and the experiment we explain by the following facts:

1. Use of  $\pi^+$  or  $\pi^-$  spectra instead of  $\pi^0$  spectra.
2. Extrapolation of the thermodynamic spectra from lower energies or small angles to energies of 1,500 GeV and the entire angular range also, in the case of the  $\pi^+$  and  $\pi^-$  spectra [6] leads to differences of the same order of magnitude from the experimental ISR data. Exact matching of the spectra with the ISR energies was not attempted in any of the cases.

We thank Mr. Magnus for support in programming; Mr. Ilgenfritz and Mr. Hatthäus for useful discussions. Not

least, we thank Mrs. Eichel for the carefully performed copy of the manuscript.

### Summary

In high-energy collisions,  $\gamma$  quanta arise from the disintegration of primarily produced  $\pi^0$  mesons. The inclusive momentum distributions of the  $\gamma$  spectra are computed through a transformation of the  $\pi^0$  spectra by means of the thermodynamic model. The work was stimulated by a group of Soviet physicists at the VIK Dubna, who performed the corresponding experiment using a propane bubble chamber at the 76 GeV accelerator at Serpuchow. The results of this experiment should be used for comparison.

### References

- [1] *Fidecaro, M., G. Finocchiaro, G. Gath, G. Giacomelli, W. C. Middelkoop und T. Yamagata*, Nuovo Cim., 24, 73, 1961.
- [2] *Grote, H., R. Hagedorn und J. Ranft*, Particle spectra, CERN 1970.
- [3] *Hagedorn, R.*, Relativistic Kinematics, New York 1964.
- [4] *Hagedorn, R.*, Suppl. Nuovo Cim., 3, 147, 1965.
- [5] *Hagedorn, R., und J. Ranft*, Suppl. Nuovo Cim., 6, 169, 1968.
- [6] *Hagedorn, R., und J. Ranft*, CERN-Preprint 1440, 1972 (in Vorb.).
- [7] *Huun Than*, unveröff. Rechnungen.
- [8] *Neuhöfer, G., F. Niebergall, J. Penzias, M. Regler, W. Schmidt-Parzefall, K. R. Schubert, P. E. Schumacher, M. Steuer und K. Winter*, CERN-Hamburg-Vienna-Collaboration, Geneva, 2. Dez. 1971, Preprint (zur Veröff. in Phys. Lett. eingeschickt).
- [9] *Ranft, J.*, Karl-Marx-University-Report TUL 37, 1970.
- [10] *Ranft, J.*, Phys. Lett., 31 B, 529, 1970.
- [11] *Sternheimer, R. M.*, Phys. Rev., 99, 277, 1955.

UNCLASSIFIED

SECURITY CLASSIFICATION OF THIS PAGE (When Data Entered)

REPORT DOCUMENTATION PAGE		READ INSTRUCTIONS BEFORE COMPLETING FORM
1. REPORT NUMBER FTD-ID(RS)T-0900-77	2. GOVT ACCESSION NO.	3. RECIPIENT'S CATALOG NUMBER
4. TITLE (and Subtitle) THE CALCULATION OF INCLUSIVE GAMMA SPECTRA AT HIGH ENERGIES	5. TYPE OF REPORT & PERIOD COVERED Translation	
	6. PERFORMING ORG. REPORT NUMBER	
7. AUTHOR(s) R. Blutner, S. Frank, et al.	8. CONTRACT OR GRANT NUMBER(s)	
9. PERFORMING ORGANIZATION NAME AND ADDRESS Foreign Technology Division Air Force Systems Command U. S. Air Force	10. PROGRAM ELEMENT, PROJECT, TASK AREA & WORK UNIT NUMBERS	
11. CONTROLLING OFFICE NAME AND ADDRESS	12. REPORT DATE 1972	
	13. NUMBER OF PAGES 17	
14. MONITORING AGENCY NAME & ADDRESS (if different from Controlling Office)	15. SECURITY CLASS. (of this report) UNCLASSIFIED	
	15a. DECLASSIFICATION/DOWNGRADING SCHEDULE	
16. DISTRIBUTION STATEMENT (of this Report) Approved for public release; distribution unlimited.		
17. DISTRIBUTION STATEMENT (of the abstract entered in Block 20, if different from Report)		
18. SUPPLEMENTARY NOTES		
19. KEY WORDS (Continue on reverse side if necessary and identify by block number)		
20. ABSTRACT (Continue on reverse side if necessary and identify by block number) 20		

DISTRIBUTION LIST

DISTRIBUTION DIRECT TO RECIPIENT

ORGANIZATION	MICROFICHE	ORGANIZATION	MICROFICHE
A205 DMATC	1	E053 AF/INAKA	1
A210 DMAAC	2	E017 AF/RDXTR-W	1
B344 DIA/RDS-3C	8	E404 AEDC	1
C043 USAMIA	1	E408 AFWL	1
C509 BALLISTIC RES LABS	1	E410 ADTC	1
C510 AIR MOBILITY R&D LAB/FIO	1	E413 ESD	2
C513 PICATINNY ARSENAL	1	FTD	
C535 AVIATION SYS COMD	1	CCN	1
C557 USAIIC	1	ETID	3
C591 FSTC	5	NIA/PHS	1
C619 MIA REDSTONE	1	NICD	5
D008 NISC	1		
H300 USAICE (USAREUR)	1		
P005 ERDA	1		
P055 CIA/CRS/ADD/SD	1		
NAVORDSTA (50L)	1		
NAVWPNSCEN (Code 121)	1		
NASA/KSI	1		
AFIT/LD	1		

